Published in final edited form as:
Int J Hyperthermia. 2013 December ; 29(8): 819–827. doi:10.3109/02656736.2013.845801.

Comparison of magnetic nanoparticle and microwave hyperthermia cancer treatment methodology and treatment effect in a rodent breast cancer model

Alicia A. Petryk, PhD,
Thayer School of Engineering, Dartmouth College, 14 Engineering Drive, Hanover, NH 03755, USA. Phone: (603) 381-535

Andrew J. Giustini, PhD,
Thayer School of Engineering, Geisel School of Medicine, Dartmouth College

Rachel E. Gottesman, BA,
Geisel School of Medicine, Dartmouth College

B. Stuart Trembly, PhD, and
Thayer School of Engineering, Dartmouth College

P. Jack Hoopes, DVM, PhD
Geisel School of Medicine, Thayer School of Engineering, Dartmouth College

Alicia A. Petryk: Alicia.A.Petryk@Dartmouth.edu

Abstract

Purpose—The purpose of this study was to compare the efficacy of iron oxide/magnetic nanoparticle hyperthermia (mNPH) and 915 MHz microwave hyperthermia at the same thermal dose in mouse mammary adenocarcinoma model.

Materials and Methods—A thermal dose equivalent to 60 minutes at 43°C (CEM 60) was delivered to a syngeneic mouse mammary adenocarcinoma flank tumor (MTGB) via mNPH or locally delivered 915 MHz microwaves. mNPH was generated with ferromagnetic, hydroxyethyl starch coated magnetic nanoparticles. Following mNP delivery, the mouse/tumor was exposed to an alternating magnetic field (AMF). The microwave hyperthermia treatment was delivered by a 915 MHz microwave surface applicator. Time required for the tumor to reach three times the treatment volume was used as the primary study endpoint. Acute pathological effects of the treatments were determined using conventional histopathological techniques.

Results—Locally delivered mNPH resulted in a modest improvement in treatment efficacy as compared to microwave hyperthermia (p=0.09) when prescribed to the same thermal dose. Tumors treated with mNPH also demonstrated reduced peritumoral normal tissue damage.

Conclusions—Our results demonstrate similar tumor treatment efficacy when tumor heating is delivered by locally delivered mNPs and 915 MHz microwaves at the same measured thermal dose. However, mNPH treatments did not result in the same type or level of peritumoral damage

Correspondence to: Alicia A. Petryk, Alicia.A.Petryk@Dartmouth.edu.

seen with the microwave hyperthermia treatments. These data suggest that mNP hyperthermia is capable of improving the therapeutic ratio for locally delivered tumor hyperthermia. These results further indicate that this improvement is due to improved heat localization in the tumor.

Keywords

Nanoparticle; Hyperthermia; Iron Oxide; Microwave; Cumulative Equivalent; Minutes

Introduction

In the past forty years, great strides have been made in understanding thermal dosimetry, treatment planning and the design of equipment used in medical hyperthermia.[1] Magnetic nanoparticles (mNP), in combination with an alternating magnetic field (AMF) are able to generate significant localized heating as well as a yet unspecified level of individual cell damage. Pre-clinical tumor studies, using intratumoral mNP delivery, have been promising, especially when combined with radiation and chemotherapy (manuscript by Petryk et al. in this volume). One of the primary reasons hyperthermia has not achieved widespread clinical use and acceptance is its inability to achieve localized tumor heating and the lack of an inherent increase of tumor cell sensitivity to heat.[2, 3, 4] The experiments presented here suggest that magnetic nanoparticle hyperthermia (mNPH) has the potential to become a more effective method of heat delivery to large tumor masses. The ability to treat individual (metastatic) cancer cells is also an area of active investigation with great promise.

Biologic effects of hyperthermia

The primary molecular targets of traditional thermal therapy are a diverse assortment of proteins. Alterations in enzymes, structures in the cytoskeleton, proteins associated with the plasma membrane, and proteins associated with DNA repair have all been observed in response to elevated temperatures.[5] The production of heat shock proteins, which assist in the refolding of damaged proteins, and the inhibition of DNA synthesis are also characteristic of cells exposed to heat.[6, 7] Both apoptosis and necrosis can be observed in tissue depending on the thermal dose.[8] Factors which influence the sensitivity of cells to hyperthermia include cell nutrient levels, as well as pH and oxygen concentration. It is also well known that heat increases the cytotoxic effect of many chemotherapeutic agents.[9–11]

915 Microwave hyperthermia

Microwave-induced hyperthermia results from the rotational motion of polar molecules, primarily water, in response to an oscillating electric field. Rotational energy is converted into heat energy through frictional losses in response to the motion of the molecules.[12] Microwave antennae for the delivery of localized medical hyperthermia were developed in the late 1970's and used for the first time in clinical medicine approximately 10 years later.[12, 13] Although significant clinical tumor response has been achieved using microwave therapy, significant side effects and inhomogeneous treatment effects have also been reported.[14–16]

Magnetic nanoparticle hyperthermia

When exposed to an AMF, mNP are believed to generate heat by one or more of the following mechanisms: 1) magnetic hysteresis, 2) eddy currents, 3) Brownian motion and 4) Néel paramagnetic switching.[17, 18] Heating properties of nanoparticles depend greatly on their composition, size and microstructure.[19] For mNP, eddy currents are not a significant contributor to tumor heating.[19, 20] The two main particle types for iron oxide based mNPH are superparamagnetic mNP (Brownian and Néel mechanisms) and ferromagnetic mNP (hysteresis losses).[21] The mNP utilized in this study have a ferromagnetic core composed of Fe_3O_4 crystals and are coated with biocompatible hydroxyethyl starch with a hydrodynamic radius of 110 nm.[18, 22] At 450 Oe (35.8 kA/m), 165 kHz these mNP demonstrate a specific absorption rate (SAR), in terms of Fe mass, of 151 (W/g Fe), as calculated by the following equation: $\mathrm{SAR}_{Fe}=\mathrm{C}\frac{\Delta \mathrm{T}}{\Delta \mathrm{t}*\mathrm{mNPc}}$, in which *C* is the specific heat capacity J/g * K and $\Delta T/_{\Delta t}$ is the initial heating slope observed and mNPc is the concentration of Fe (g Fe/g medium).[23,24]

Thermal dose

It is well understood that the biomedical effects of heat are a function both of time and temperature. Therefore, accurately predicting and prescribing treatment for various animal species and tissue is difficult without a means of comparing the thermal histories. Sapareto and Dewey proposed a method to normalize hyperthermia treatments conducted in different settings by describing the biologic effect in terms of cumulative equivalent minutes at 43°C (CEM).[25] The CEM relationship is: $CEM = tR^{43°C-T}$, where "t" is equal to the time interval at a specific temperature "T," *R* equals 0.25 when temperatures are below 43°C and 0.45 when temperatures are above 43°C.[26] The total thermal dose is equivalent to the summation of these values.

It is important to note that the CEM relationship, for thermal dose equivalency in tissue, has only been assessed for conventional forms of hyperthermia therapy such as microwave, ultrasound and RF- based platforms. It has not been assessed or proven for a modality such as mNPH where the heat source(s) are contained within and immediately outside of cells (cell membrane and interstitium) and the achieved temperature, on the macro-nano scale are not known. Furthermore, it is possible that the mNP heat mechanism of action is not based on heating alone.[27, 28] In the following experiments, the validity of the CEM relationship for mNPH was explored by comparing "traditional" 915 MHz hyperthermia with mNP hyperthermia. Although not specifically examined in this work, the intracellular location of mNP, as well as the grouping of the mNP within the cells, may result in improved biologic (therapeutic) effects beyond those expected with tissue-level applications of hyperthermia. Although reports of improved mNP heating and/or cytotoxicity following intracellular mNP initiated hyperthermia have been published, the issue remains unresolved and controversial.[24, 27–37] In this work, the mNP were activated within 10 minutes of injection into the tumor. Previous studies from our group suggest that mNP are largely extracellular at this time.[31] A qualitative, TEM-based, evaluation of tumors indicates that the majority of mNP are extracellular at the time of AMF initiation.

Materials and Methods

Breast Cancer Cells

Mouse mammary adenocarcinoma (MTGB) cells were grown in Alpha MEM media (Mediatech, Inc., Manassas, VA). The Alpha MEM media was modified with the addition of FBS (HyClone Laboratory, Inc., South Logan, UT) 10%, penicillin-streptomycin (HyClone Laboratory, Inc., South Logan, UT) 1%, and L-glutamine (Mediatech, Inc., Manassas, VA) 1%.

Animal Model

Syngeneic, MTGB tumors were grown in the flanks of female C3H mice (Charles River Laboratories International, Inc. Wilmington, MA) aged 6–8 weeks. Cultured MTGB cells were treated with 0.25% trypsin in EDTA (HyClone Laboratory, Inc., South Logan, UT). Cells were then suspended in unmodified Alpha MEM media, with a 50 μl sample taken for trypan blue assay evaluation. Cells were stained with trypan blue (Hyclone Laboratories, Inc.), in a 1:1 ratio and counted using a hemocytometer (Fisher Scientific, Inc., Pittsburg, PA, USA). Cells were pelleted through centrifugation and resuspended in unmodified Alpha MEM media at 10 million cells per mL.1 million cells were injected with a 25 gauge needle into the right rear flank of the mice. After 2–3 weeks, the tumors reached a volume of 150 mm^3 +/− 40 mm^3, at which time they were treated in the method described below. Tumors were measured with digital calipers in three planes. Volumes were calculated using the measured perpendicular diameters “d” of the ellipsoidal tumors and the equation:

$Volume = \frac{\pi d_1 d_2 d_3}{6}$. Following treatment, tumors were measured every other day until the volumes were three times the pretreatment volumes. The length of time from treatment until the tumor reached three times its pretreatment volume is the primary study endpoint for study efficacy.

mNP injection and dosimetry

The mNPs used in this study are Bionized NanoFerrite (BNF) nanoparticles (MicroMod GmBH Rostock, Germany), suspended in water without any surfactants, and heat via magnetic hysteresis when an AMF is applied.

The mNP were suspended at a total mNP concentration of 42 mg/mL (28 mg of Fe/mL). Intratumoral injections, in four equal quadrants, were performed using two needle tracks, at a dose of 7.5 mg of Fe per cm^3 of tumor. The average total dose of Fe per mouse was 1.2+/− 0.2 mg Fe per mouse (0.05 +/− 0.006 mg Fe per gram body weight). AMF activation was performed ten minutes following injection.

Administration of AMF

The AMF field was generated by a water cooled, whole body circular coil (Fluxtrol Inc., Auburn Hills, MI). The 5.0 cm long coil is comprised of 8 mm square tubing with 5 turns resulting in an internal diameter of 3.6 cm. The coil was powered by a Huttinger TIG 10/300 generator (Freiburg, Germany), produces an AMF field of 165 kHz and 450 Oe (35.8 kA/m). Both the coil and the generator were cooled with water at 30° C (chiller TKD250,

Tek-Temp Instruments Inc., Croydon, PA). Mice were treated under anesthesia using 1–3% isoflurane gas and 95% O^2 with an average rectal temperature of 37.5°C +/− 0.5° C.

Administration of Microwave

The microwave applicator consists of an open-ended pair of coaxial conductors, driven by a 915 MHz microwave generator and cooled by circulating water. The applicator was sized to fit the mouse flank tumor. A water based tissue equivalent coupling gel, which accommodated tumor geometry variations, was placed between the applicator and the tumor surface.[38] Mice were treated under anesthesia with an average rectal temperature of 35.7°C +/− 1.5° C.

Temperature Recording and Thermal Dose

Tumor and mouse core (rectal) temperatures were measured throughout the treatment at the center of the tumor. CEM values were calculated continuously in real-time. FISO fiber optic probes (FISO Inc., Quebec, Canada) and FISO Evolution software assessed temperatures at a rate of 1 Hz and continuously updated the measured temperatures and CEM values. Treatments were terminated when the thermal dose reached CEM 60.

The measured thermal histories for tumors treated with mNPH and 915 MHz were similar. The majority of tumors for both treatment types achieved a thermal dose of CEM 60 within 20 minutes of treatment (12 tumors for mNPH and 11 tumors for 915 MHz hyperthermia). Some tumors took longer than 20 minutes to achieve a thermal dose of CEM 60 (3 for mNPH and 6 for 915 MHz hyperthermia). Minor tumor geometry and/or mNP biodistribution variations resulted in slightly different heating rates (relationship of heating time and temperature). These differences did not meaningfully affect treatment efficacy. Some variation between treatment groups was also apparent both at the initiation and conclusion of treatment. The surface applicator used for 915 MHz microwave hyperthermia was water cooled. This design results in the initial tumor temperatures to be slightly lower for the microwave treated tumors than for the mNP treated tumors. Additionally, mNPH treated tumors retained an elevated temperature slightly longer than 915 MHz treated tumors once the field was removed.

Efficacy Treatment Groups

Four groups were evaluated for treatment efficacy (time to tumor regrowth) including: 1) mNP+AMF (n=6), 2) 915 MHz microwave (n=8), 3) AMF alone, and 4) No Treatment (n=6). Groups 1, 3 and 4 are included in an accompanying manuscript. All tumors receiving hyperthermia were treated to CEM 60. Animals treated with 915 MHz microwave hyperthermia or AMF alone received an intratumoral injection of phosphate buffered saline (PBS), at a volume equivalent to the prescribed volume of mNP. AMF control animals were exposed to 450 Oe (35.8 kA/m), 165 kHz for 30 min.

Efficacy Endpoints and Statistics

Regardless of the study arm, all mice were sacrificed when the tumor volume reached three times treatment volume. This information was analyzed for statistical significance with the

two-tailed, two-sample t-test (ttest2 function) present in the Matlab software (version R2011a, The Mathworks, Inc., Natick, MA).

Histological Evaluation

To determine the histopathological effects of the mNPH and microwave treatments, a subset of tumors (mNPH = 9, 915 MHz microwave hyperthermia = 9) were evaluated histopathologically 24 hours following treatment. The tumors were fixed in neutral buffered 10% formaldehyde and processed for standard histological slide preparation. Histologic sections were cut four microns apart and stained with hematoxylin and eosin (H&E). Qualitative and quantitative histologic analysis and photomicroscopy were performed using conventional light microscopy and the NIH open source “Image J” quantification software (NIH, Bethesda, MD). The tumor treatment effects (live vs. necrotic) was determined by tracing the total tumor area and the area of necrosis. The level of normal tissue injury beneath the tumor was determined by establishing zones 0.75, 1.5 and 2.25 mm beneath the tumor. Each zone was morphologically evaluated for the presence of edema, hemorrhage and muscle necrosis.

Results

mNP treated tumors had a 31% increase in regrowth delay (21 vs. 16 days) as compared to microwave treated tumors at the same thermal dose. Student’s t-tests demonstrated statistical significance of $p=0.09$.

The mNP treatments demonstrated large regions of necrosis as well as focal necrosis and hemorrhage. Although tumors were largely necrotic 24 hours following treatment, small regions of morphologically viable cells were noted near the tumor boundary. Although unclear from microscopic observation, these regions of viability were likely associated with low levels of mNP coverage. Moderate peritumor edema was also noted in a few mNPH treated tumors. However, peritumor muscle necrosis and hemorrhage was not observed.

Tumors treated with 915 MHz microwave hyperthermia demonstrated distinct regions of necrosis and cell viability. Viable cells were typically seen in the superficial and lateral tumor region. Additional histologic evaluation of the surrounding normal tissue noted the presence of peritumor edema, mild inflammation and underlying muscle necrosis.

Histologic evaluation of the mNP and microwave treated tumor demonstrated distinctly different patterns of necrosis and viability. Although the measured thermal dose for mNPH and microwave treatments was approximately the same, the presence of scattered focal zones of cell damage within an individual tumor following mNPH suggests that the mNP distribution and resulting tumor heating was not uniform. This information highlights the importance of mNP dose and biodistribution in the tumor with respect to delivered thermal dose, treatment effect and safety.

Discussion

mNP delivered via direct injection to the tumor volume was distributed to the majority of the tumor primarily along fascial planes, providing a controlled, effective and reproducible thermal dose. While the mNPH and microwave hyperthermia treatment effects and thermal dose are similar for our mouse tumor model, the data suggest that mNPH is slightly more effective ($p=0.09$) from a tumor regrowth analysis standpoint. Since the AMF exposure was completed shortly following mNP delivery, the degree of cellular uptake was small. Therefore, the generated heat is primarily extracellular, although further investigation and quantification of mNP uptake or distribution changes during AMF exposure is necessary. Whether the molecular targets of nanoparticle-based hyperthermia are different, or can be made different, using the intracellular potential of mNP, remains unclear and will require additional studies utilizing well documented mNP location parameters.[39]

Although histologic evaluation of the treated tumor tissues indicated relatively minor differences in the level of tumor necrosis/treatment efficacy for mNPH and 915 MHz microwave hyperthermia, significantly less peritumor normal tissue damage was observed in tumors treated with mNPH. Since normal tissue effects limit the tolerated dose of all cancer therapies, our results suggest that the improved geometric confinement of mNP hyperthermia to the tumor volume may offer significant advantages over conventional local hyperthermia techniques, where the energy waves are not greatly confined by various tumor and non-tumor tissue boundaries.

While our study suggests that when mNP are primarily extracellular at the initiation of treatment, that mNPH may not be significantly more efficacious than “traditional” hyperthermia of the same thermal dose, it does indicate that mNPH may be more effective at delivering a uniform thermal dose, to a target volume. As the specific geometry of each clinical tumor is unique, this study also indicates that mNP may be better at sparing the sensitive and often dose limiting normal tissue which surrounds a tumor. If mNP can be further targeted to tumor and tumor cells through tumor antibody directed mNP, and/or static magnetic fields, the therapeutic ratio may be further improved.[40] Furthermore, the development and use of mNP imaging prior to activation will not only allow for real time determination of mNP distribution, but will also allow for improved treatment planning.[41, 42] If accurate and reproducible mNP treatment planning, based on mNP SAR, mNP concentration, location and field strength can be realized, the dependence on invasive thermal measurements may be reduced or even eliminated. This situation would enable more cost and time efficient treatments without sacrificing safety or efficacy.

Conclusion

These experiments demonstrate a similar therapeutic effect in a mouse mammary adenocarcinoma model for locally delivered intratumoral mNPH at 7.5 mg Fe/gram tumor and 915 MHz microwave hyperthermia at the same thermal dose (CEM 60). This finding suggests that, for acutely activated, locally delivered mNP, that the CEM relationship remains a valid method for prescribing a tumor treatment and delivering a quantifiable and meaningful thermal dose. Similar studies have not yet been conducted for intracellular

mNPH. Additionally, the accurate measurement of intracellular mNP, following AMF activation, remains challenging. With these factors in mind, it remains possible that significant thermal effects in tumors can be achieved at measured temperatures and thermal doses previously believed to be too low to result in tumor cytotoxicity. Following treatment, histopathological examination of tumor and the surrounding tissue show reduced normal tissue damage for mNPH as compared to 915 MHz hyperthermia. As such, we propose mNPH has the potential for improved clinical safety and efficacy, as compared to conventional (microwave, radiofrequency, etc.) local hyperthermia treatment techniques.

Acknowledgments

Declaration of Interests:

This work was supported by the Dartmouth Center of Cancer Nanotechnology Excellence (National Institutes of Health National Cancer Institute grant 1U54CA151662-01). A.A.P. and A.J.G. gratefully acknowledge support from the Thayer School of Engineering Innovation Fellowship. We would also like to thank Rendall Strawbridge for his assistance with the animal model and Louisa Howard for her TEM imaging contributions.

References

1. Hurwitz MD. Today's thermal therapy: Not your father's hyperthermia: Challenges and opportunities in application of hyperthermia for the 21st century cancer patient. Am J Clin Oncol. 2010; 33(1):96–100. [PubMed: 19636240]
2. Roizin-Towle L, Pirro JP. The response of human and rodent cells to hyperthermia. Int J Radiat Oncol Biol Phys. 1991; 20(4):751–756. [PubMed: 2004951]
3. Lagendijk J. Hyperthermia treatment planning. Phys Med Biol. 2000; 45(5):R61–R76. [PubMed: 10843091]
4. Review of tumor hyperthermia technique in biomedical engineering frontier; Biomedical engineering and informatics (BMEI), 2010 3rd international conference on IEEE; 2010.
5. Hall, EJ. Radiobiology for the radiologist. 5th ed.. Philadelphia: Lippincott Williams & Wilkins; 2000.
6. Hildebrandt B, Wust P, Ahlers O, Dieing A, Sreenivasa G, Kerner T, Felix R, Riess H. The cellular and molecular basis of hyperthermia. Crit Rev Oncol. 2002; 43(1):33–56.
7. Streffer C. Review: Metabolic changes during and after hyperthermia. Int J Hyperthermia. 1985; 1(4):305–319. [PubMed: 2425020]
8. Harmon B, Corder A, Collins R, Gobe G, Allen J, Allan D, Kerr J. Cell death induced in a murine mastocytoma by 42–47 C heating in vitro: Evidence that the form of death changes from apoptosis to necrosis above a critical heat load. Int J Radiat Biol. 1990; 58(5):845–858. [PubMed: 1977828]
9. Hahn GM, Shiu EC. Effect of pH and elevated temperatures on the cytotoxicity of some chemotherapeutic agents on chinese hamster cells in vitro. Cancer Res. 1983; 43(12 Part 1):5789. [PubMed: 6196107]
10. Overgaard J, Bichel P. The influence of hypoxia and acidity on the hyperthermic response of malignant cells in vitro. Radiology. 1977; 123(2):511–514. [PubMed: 15300]
11. Hahn GM. Hyperthermia for the engineer: A short biological primer. IEEE Trans Biomed Eng. 1984; (1):3–8. [PubMed: 6724607]
12. Trembly, BS.; Ryan, TP.; Strohbehn, JW. Physics of microwave hyperthermia. In: Urano, M.; Douple, E., editors. Hyperterhmia and oncology: Theramal effects on cells and tissues. The Netherlands: VSP BV; 1992.
13. Coughlin, CT. Interstitial hyperthermia: Physics, biology and clinical aspects. CRC Press; 1992.
14. Lindholm C, Kjellen E, Nilsson P, Hertzman S. Microwave-induced hyperthermia and radiotherapy in human superficial tumours: Clinical results with a comparative study of combined treatment versus radiotherapy alone. International Journal of Hyperthermia. 1987; 3(5):393–411. [PubMed: 3681040]

15. Vargas HI, Dooley WC, Gardner RA, Gonzalez KD, Venegas R, Heywang-Kobrunner SH. Focused microwave phased array thermotherapy for ablation of early-stage breast cancer: Results of thermal dose escalation. Annals of Surgical Oncology. 2004; 11(2):139–146. [PubMed: 14761916]

16. Dooley WC, Vargas HI, Tomaselli MB, Harness JK. Focused microwave thermotherapy for preoperative treatment of invasive breast cancer: A review of clinical studies. Annals of Surgical Oncology. 2010; 17(4):1076–1093. [PubMed: 20033319]

17. Giustini AJ, Petryk AA, Cassim SM, Tate JA, Baker I. Magnetic nanoparticle hyperthermia in cancer treatment. Nano LIFE. 2010; 1&2:17.

18. Dennis C, Jackson A, Borchers J, Hoopes P, Strawbridge R, Foreman A, Van Lierop J, Grüttner C, Ivkov R. Nearly complete regression of tumors via collective behavior of magnetic nanoparticles in hyperthermia. Nanotechnology. 2009; 20(39):395103. [PubMed: 19726837]

19. Hergt R, Andra W, d'Ambly CG, Hilger I, Kaiser WA, Richter U, Schmidt H. Physical limits of hyperthermia using magnetite fine particles. Magnetics, IEEE Transactions On. 1998; 34(5):3745–3754.

20. Etheridge, M.; Manuchehrabadi, N.; Franklin, R.; Bischoff, J. Superparamagnetic iron oxide nanoparticle heating: A basic tutorial. In: Minkowycz, WJ.; Sparrow, EM.; Abraham, JP., editors. Nanoparticle heat transfer and fluid flow. CRC Press; 2012.

21. Etheridge, M.; Jordan, A.; Bischof, JC. Magnetic nanoparticles for cancer therapy. In: Moros, Eduardo, editor. Physics of thermal therapy: Fundamentals and clinical applications. Taylor & Francis: 2012.

22. Grüttner C, Müller K, Teller J, Westphal F, Foreman A, Ivkov R. Synthesis and antibody conjugation of magnetic nanoparticles with improved specific power absorption rates for alternating magnetic field cancer therapy. J Magn Magn Mater. 2007; 311(1):181–186.

23. Mornet S, Vasseur S, Grasset F, Duguet E. Magnetic nanoparticle design for medical diagnosis and therapy. J Mater Chem. 2004; 14(14):2161–2175.

24. Etheridge M, Bischof J. Optimizing magnetic nanoparticle based thermal therapies within the physical limits of heating. Ann Biomed Eng. 2013; 41(1):78–88. [PubMed: 22855120]

25. Sapareto SA, Dewey WC. Thermal dose determination in cancer therapy. Int J Radiat Oncol Biol Phys. 1984; 10(6):787–800. [PubMed: 6547421]

26. Dewhirst MW, Viglianti BL, Lora-Michiels M, Hanson M, Hoopes PJ. Basic principles of thermal dosimetry and thermal thresholds for tissue damage from hyperthermia. Int J Hyperthermia. 2003; 19(3):267,267–294. [PubMed: 12745972]

27. Duguet E, Hardel L, Vasseur S. Cell targeting and magnetically induced hyperthermia. Thermal Nanosystems and Nanomaterials (Topics in Applied Physics). 2009; 118:343.

28. Creixell M, Bohórquez AC, Torres-Lugo M, Rinaldi C. EGFR-targeted magnetic nanoparticle heaters kill cancer cells without a perceptible temperature rise. ACS Nano. 2011; 5(9):7124–7129. [PubMed: 21838221]

29. Rodríguez-Luccioni HL, Latorre-Esteves M, Méndez-Vega J, Soto O, Rodríguez AR, Rinaldi C, Torres-Lugo M. Enhanced reduction in cell viability by hyperthermia induced by magnetic nanoparticles. Int J Nanomedicine. 2011; 6:373–380. [PubMed: 21499427]

30. Jordan A, Wust P, Scholz R, Tesche B, Fähling H, Mitrovics T, Vogl T, Cervos-Navarro J, Felix R. Cellular uptake of magnetic fluid particles and their effects on human adenocarcinoma cells exposed to AC magnetic fields in vitro. Int J Hyperthermia. 1996; 12(6):705–722. [PubMed: 8950152]

31. Giustini A, Ivkov R, Hoopes P. Magnetic nanoparticle biodistribution following intratumoral administration. Nanotechnology. 2011; 22(34):345101. [PubMed: 21795772]

32. Moroz P, Jones S, Gray B. Magnetically mediated hyperthermia: Current status and future directions. Int J Hyperthermia. 2002; 18(4):267–284. [PubMed: 12079583]

33. Fortin J, Gazeau F, Wilhelm C. Intracellular heating of living cells through néel relaxation of magnetic nanoparticles. Eur Biophys J. 2008; 37(2):223–228. [PubMed: 17641885]

34. Hedayati M, Thomas O, Abubaker-Sharif B, Zhou H, Cornejo C, Zhang Y, Wabler M, Mihalic J, Gruettner C, Westphal F. The effect of cell cluster size on intracellular nanoparticle-mediated

hyperthermia: Is it possible to treat microscopic tumors? Nanomedicine. 2013; 8(1):29–41. [PubMed: 23173694]

35. Gordon R, Hines J, Gordon D. Intracellular hyperthermia a biophysical approach to cancer treatment via intracellular temperature and biophysical alterations. Med Hypotheses. 1979; 5(1): 83–102. [PubMed: 459972]
36. Giustini AJ, Hoopes PJ, Gottesman RE, Petryk AA, Rauwerdink AM. Kinetics and pathogenesis of intracellular magnetic nanoparticle cytotoxicity. Proc of SPIE. 2011 SPIE BiOS: 790118-1,790118-7.
37. Rabin Y. Is intracellular hyperthermia superior to extracellular hyperthermia in the thermal sense? Int J Hyperthermia. 2002; 18(3):194–202. [PubMed: 12028637]
38. Trembly BS. Microwave thermal keratoplasty for myopia: Keratoscopic evaluation in porcine eyes. Journal of Refractive Surgery. 1995; 17(6):682. [PubMed: 11758987]
39. Dennis C, Jackson A, Borchers J, Ivkov R, Foreman A, Hoopes P, Strawbridge R, Pierce Z, Goerntiz E, Lau J. The influence of magnetic and physiological behaviour on the effectiveness of iron oxide nanoparticles for hyperthermia. J Phys D. 2008; 41(13):134020.
40. Targeting of systemically-delivered magnetic nanoparticle hyperthermia using a noninvasive, static, external magnetic field. SPIE BiOS International Society for Optics and Photonics. 2013
41. Thiesen B, Jordan A. Clinical applications of magnetic nanoparticles for hyperthermia. Int J Hyperthermia. 2008; 24(6):467–474. [PubMed: 18608593]
42. Hoopes PJ, Petryk AA, Gimi B, Giustini AJ, Weaver JB, Bischof J, et al. In vivo imaging and quantification of iron oxide nanoparticle uptake and biodistribution. SPIE Medical Imaging. 2012 83170R-83170R.

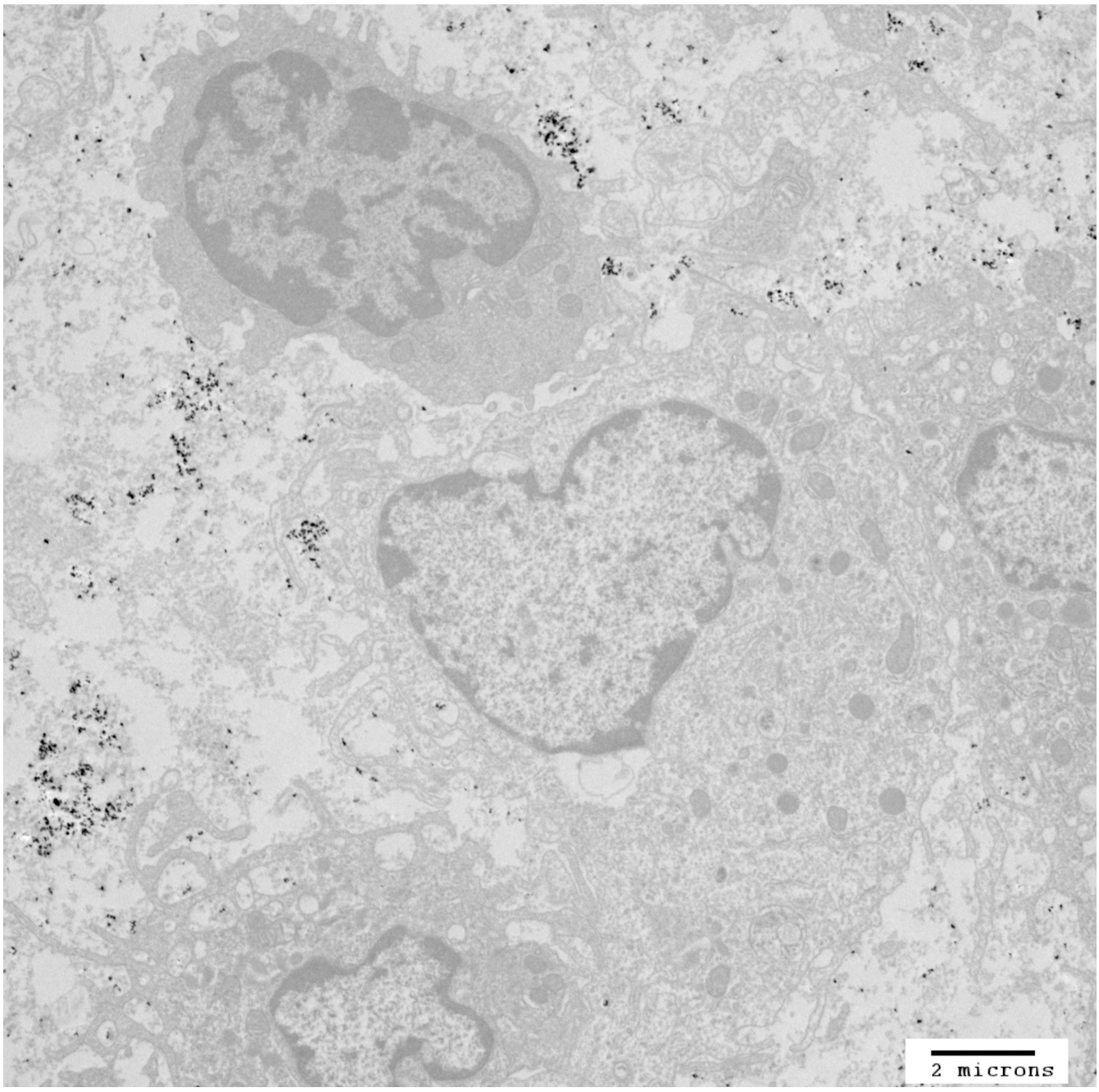

Figure 1.

TEM image of mNP associated with murine mammary adenocarcinoma (MTGB) tumor cells. This section was acquired 5 minutes following delivery of 7.5 mg Fe/cm^3 directly into the MTGB tumor mass. mNP (black specs) are located between cells (interstitial space), attached to the exterior aspect of the cell plasma membrane or in membrane associated vesicles. Scale bar = 2μm. Qualitative evaluation of tumors (n=4), harvested at the prescribed treatment time, indicate that the mNP distribution at the initiation of AMF is dominated by extracellular mNP.

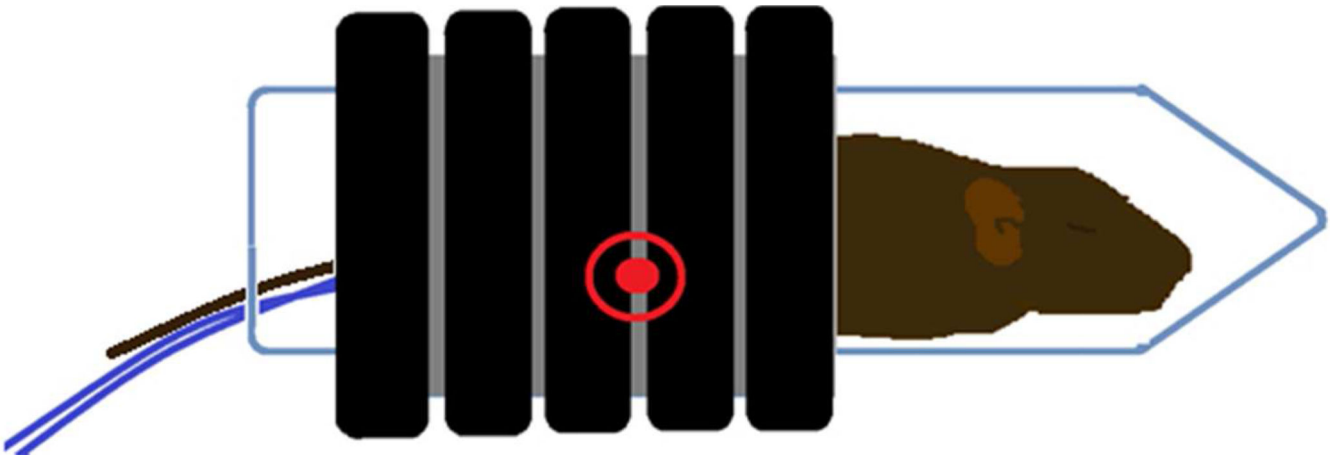

Figure 2.

This figure demonstrates the techniques used to deliver the alternating magnetic field (AMF) to a tumor bearing mouse. The AMF field was generated by a water cooled, whole body circular coil which produced an AMF field of 165 KHz and 450 Oe (35.8 kA/m). The location of the flank based tumor within the coil is indicated by the red encircled dot. This region demonstrates a near uniform, homogenous AMF. The tumor temperatures and core temperature of the mouse were measured throughout the treatment using real time fiber optic thermometry. The thermal history of the treatment was continuously calculated and displayed for the tumor and body core throughout the experimental period.

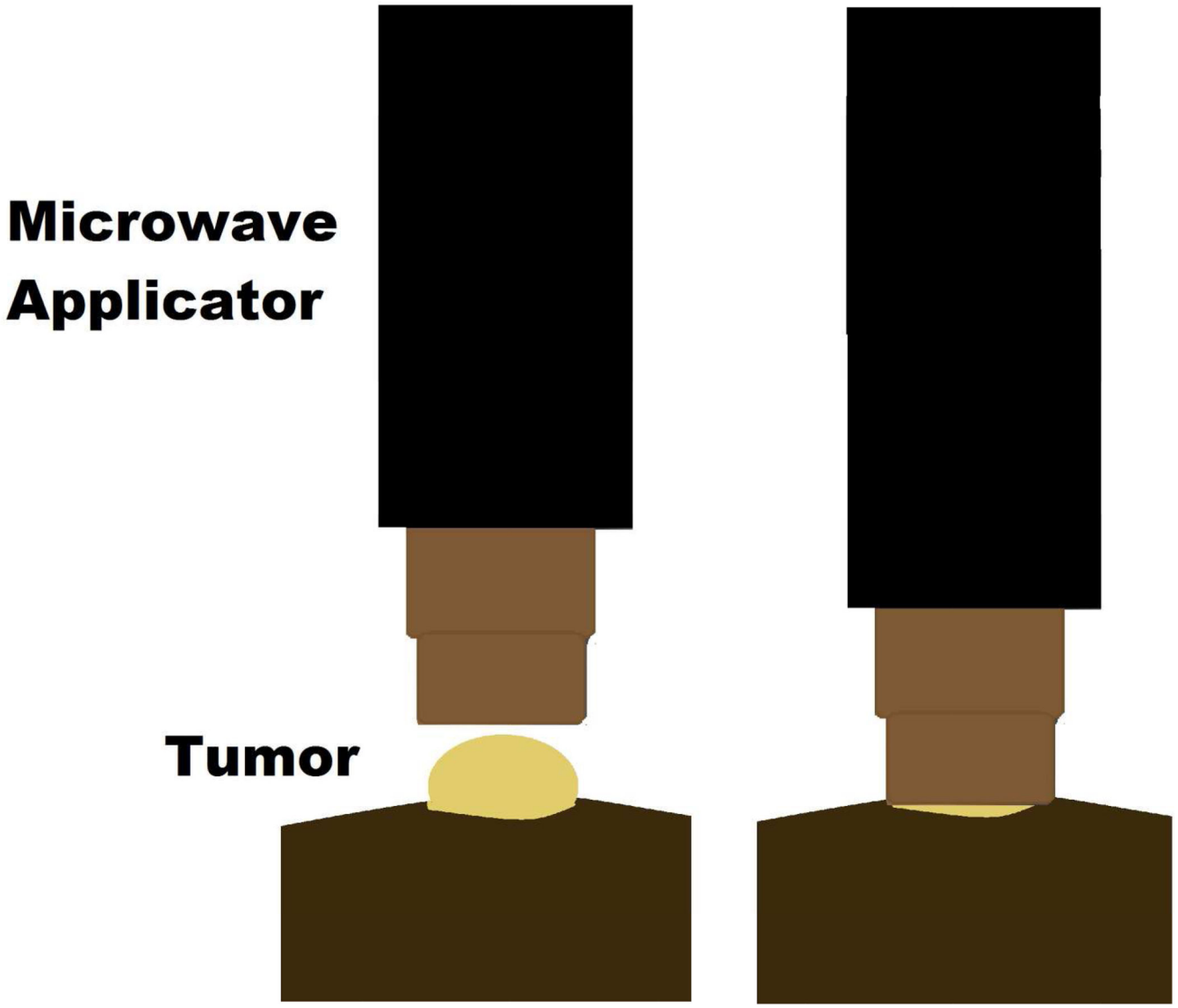

Figure 3.

The microwave applicator used for tumor treatments consist of an open-ended pair of coaxial conductors, which was driven by a 915 MHz microwave generator, cooled by circulating water and sized to fit over the flank tumor of the mice. Tissue-applicator coupling gel was placed between the applicator and the tumor surface. Tumor temperatures and core temperature of the mice were measured throughout the treatment, with thermal history (CEM) calculated in real-time.

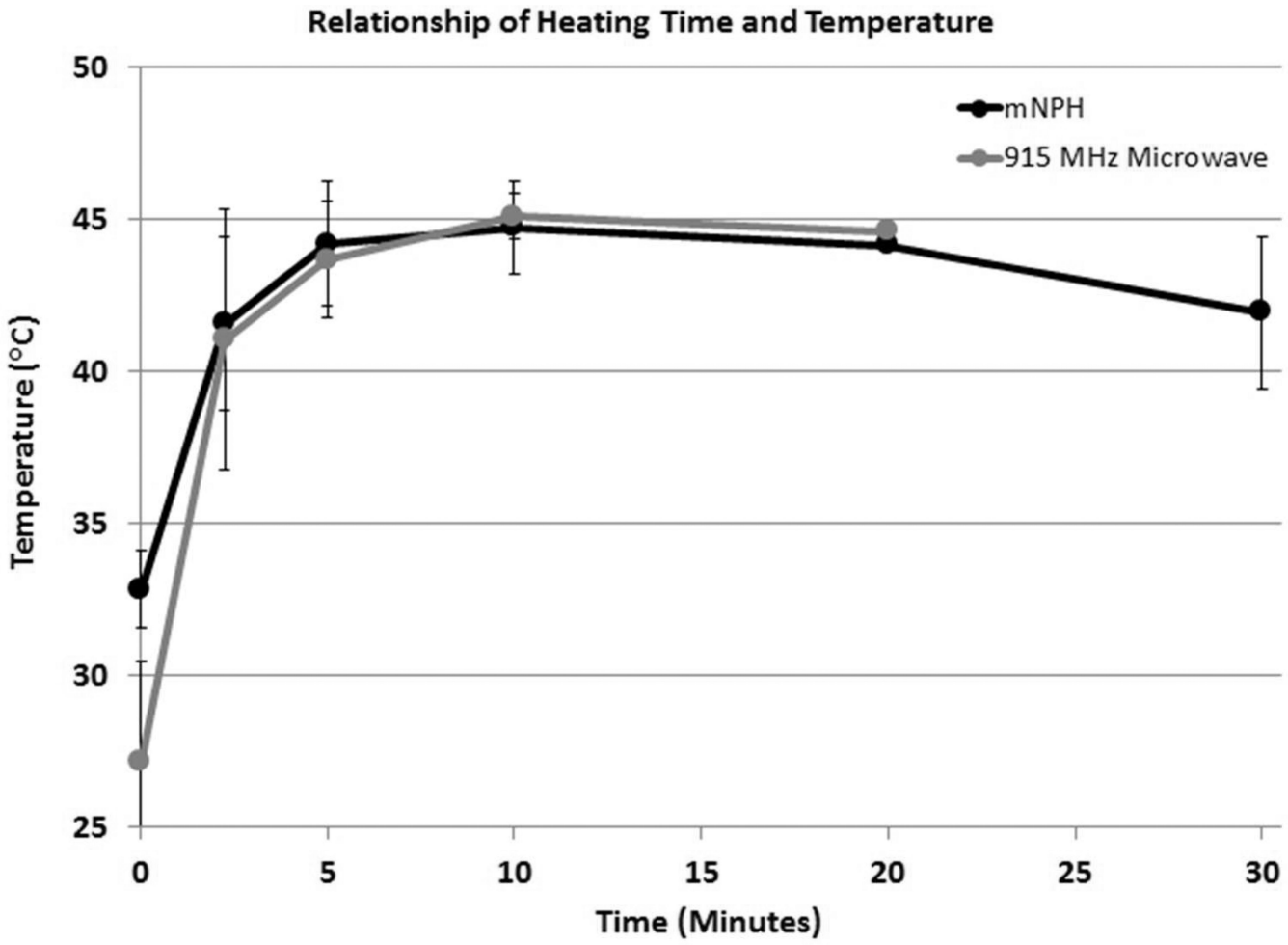

Figure 4.

This graph demonstrates the tumor heating characteristics for the mNPH and microwave treatment modalities. All tumors received a thermal dose equal to 60 minutes at 43°C (CEM 60). Minor tumor geometry and/or mNP biodistribution variations resulted in slightly different heating rates (relationship of heating time and temperature). These differences did not meaningfully affect treatment efficacy.

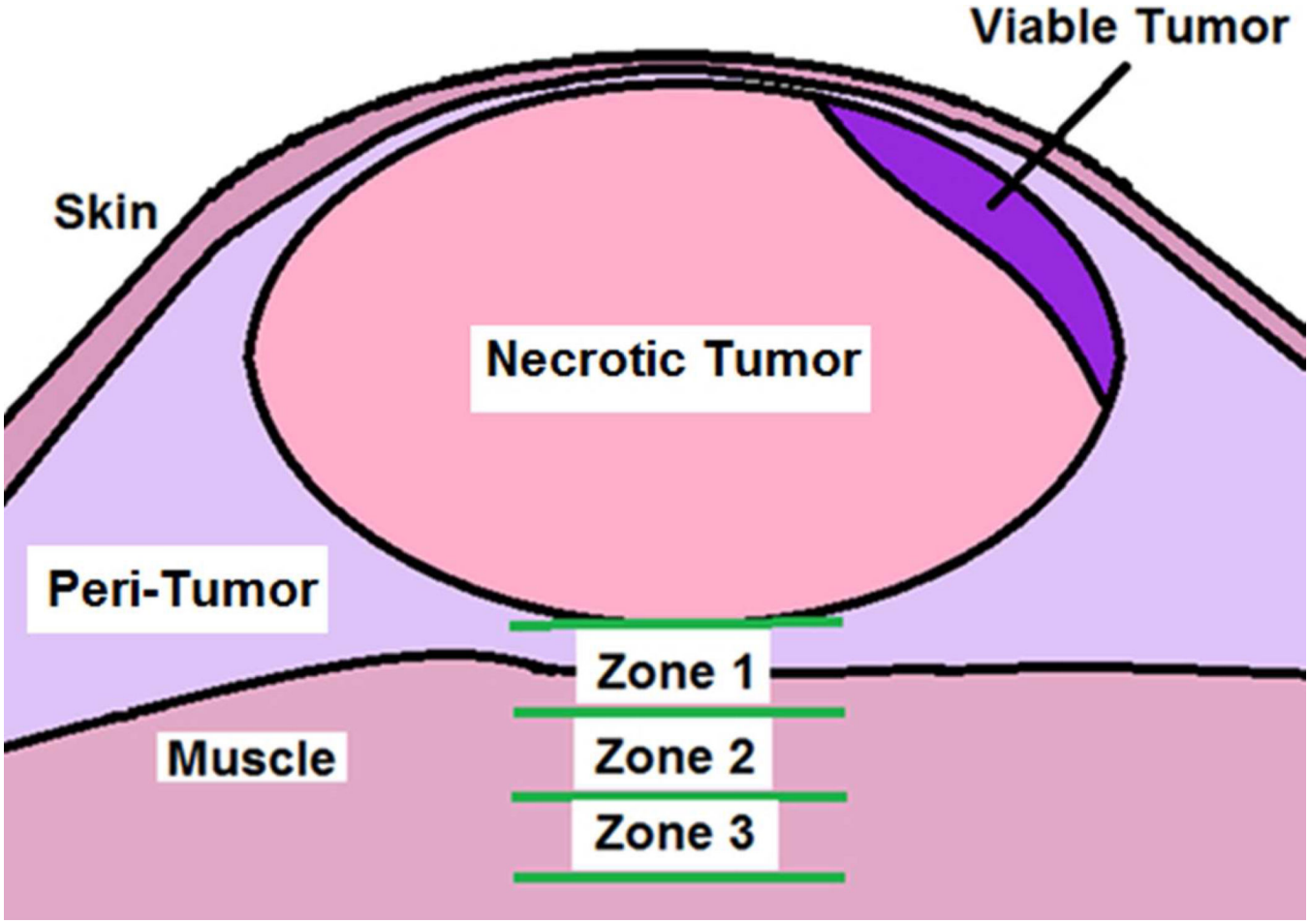

Figure 5.

This figure represents the histological parameters used to assess a treated mouse tumor and associated normal tissue deep to the tumor. Zones 1, 2 and 3 were used to determine and quantify the morphological tissue response at various depths beneath the tumor following treatment. Each zone had a thickness of 0.75 mm. Zone 1 started at the deep edge of the tumor. A quantitative cross-sectional area method was used to determine the relative amount of viable vs. non-viable tumor area. The presence of normal tissue/muscle necrosis, peritumoral edema and/or hemorrhage was categorized for each of the three zones for each tumor.

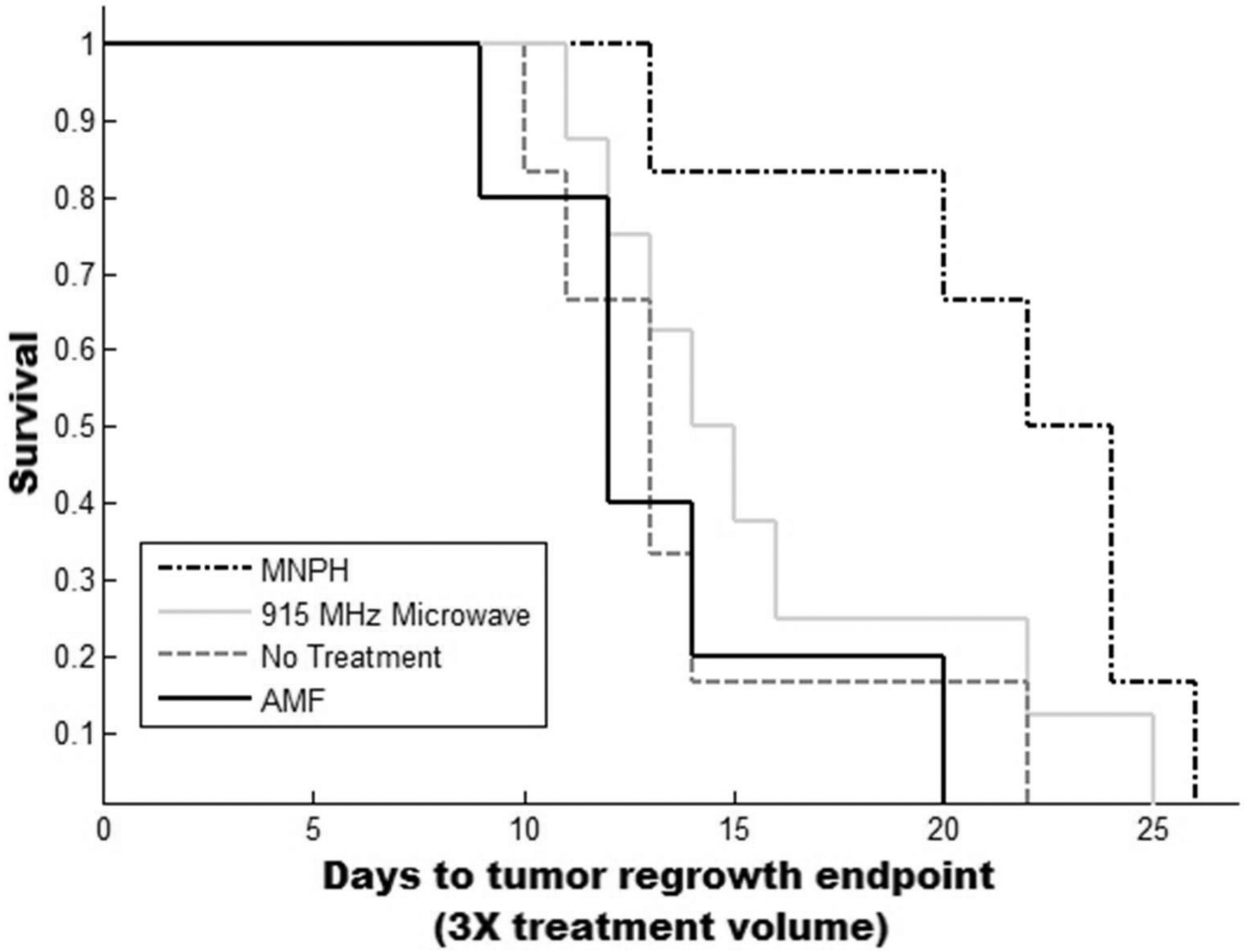

Figure 6.

Kaplan-Meyer curve demonstrating survival/tumor regrowth for each of the four treatment groups (No Treatment, AMF, mNPH and 915 MHz microwave hyperherthermia). Tumors were treated at 150 mm^3 +/− 40 mm^3. Animals were removed from the study when tumor volumes reached a three fold treatment volume increase. Treatment with mNP hyperthermia resulted in a slightly more effective treatment than 915 MHz microwave hyperthermia (p=0.09, 5 days).

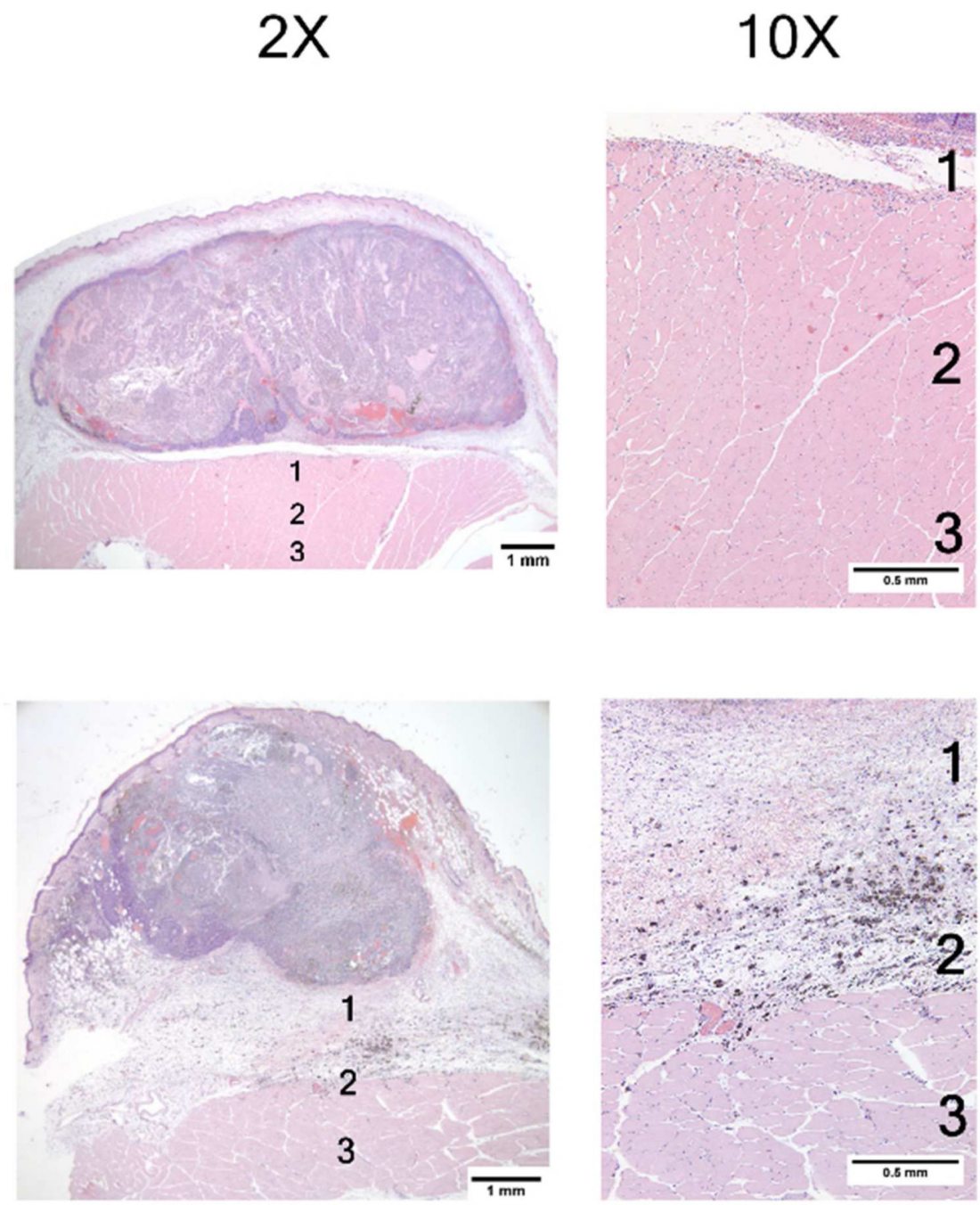

Figure 7.

These photomicrographs acquired 24 hours post mNPH treatment, demonstrate the morphological changes observed in two different tumors which received an identical thermal dose (CEM 60). Both tumors show extensive uniform necrosis. The lower tumor demonstrates significant edema in the space between the tumor and underlying muscle (Zones 1 and 2). Although minor inflammation is seen, including mNP-containing macrophages, there was no hemorrhage or necrosis in the overlying skin or peritumoral tissue.

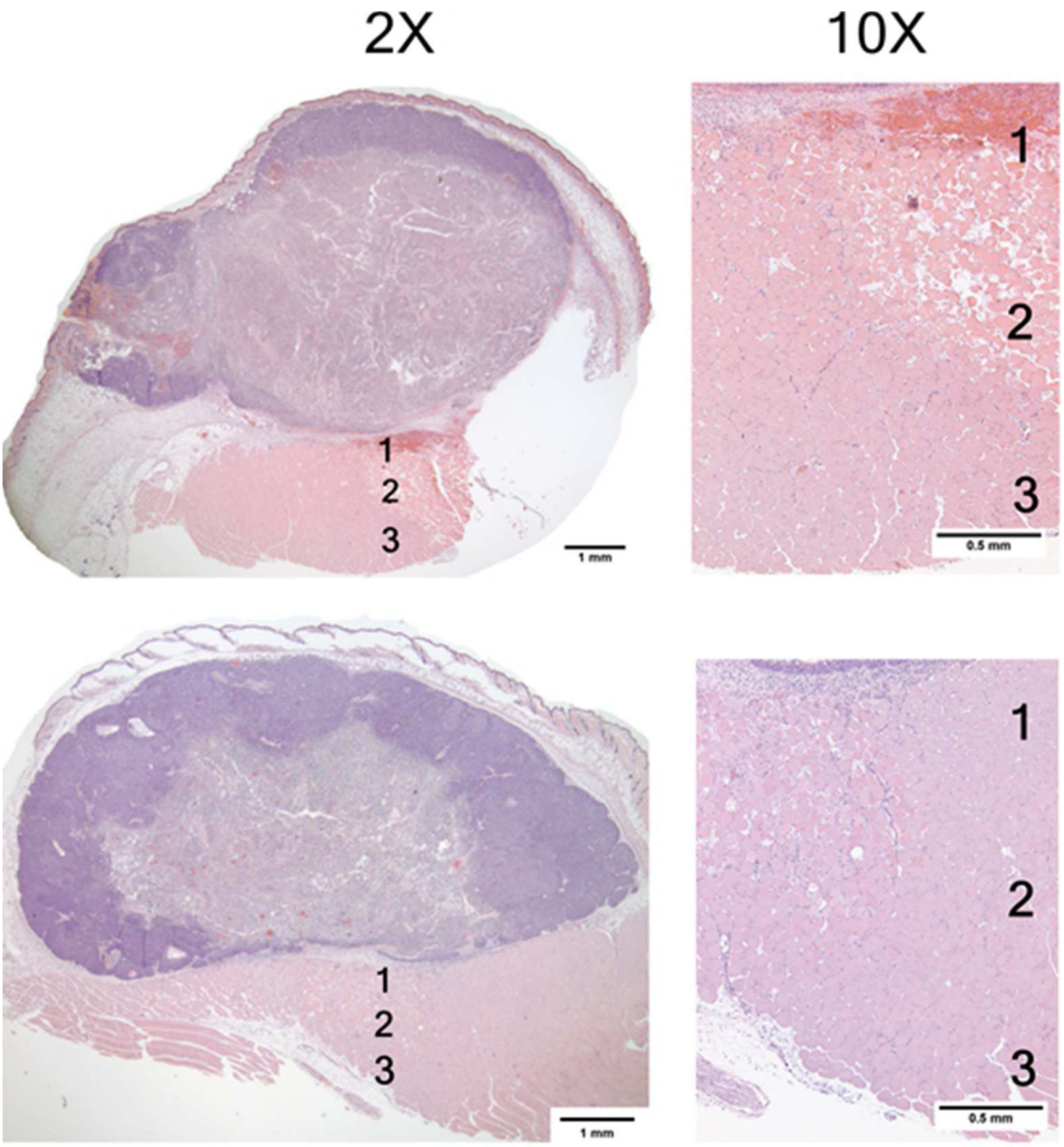

Figure 8.

Photomicrographs of two mouse mammary tumors 24 hours post 915 microwave treatment. These photomicrographs show similar effects consisting largely of generalized central tumor necrosis. The superfical tumor is spared, likely due to applicator cooling. The high magnification (10×) photomicrographs of muscle tissue deep to the tumor demonstrate varying degress of muscle necrosis, hemorrhage and inflammation. The majority of the changes are seen in Zones 1 and 2. See Figure 5 for information on tissue damage quantification techniques.

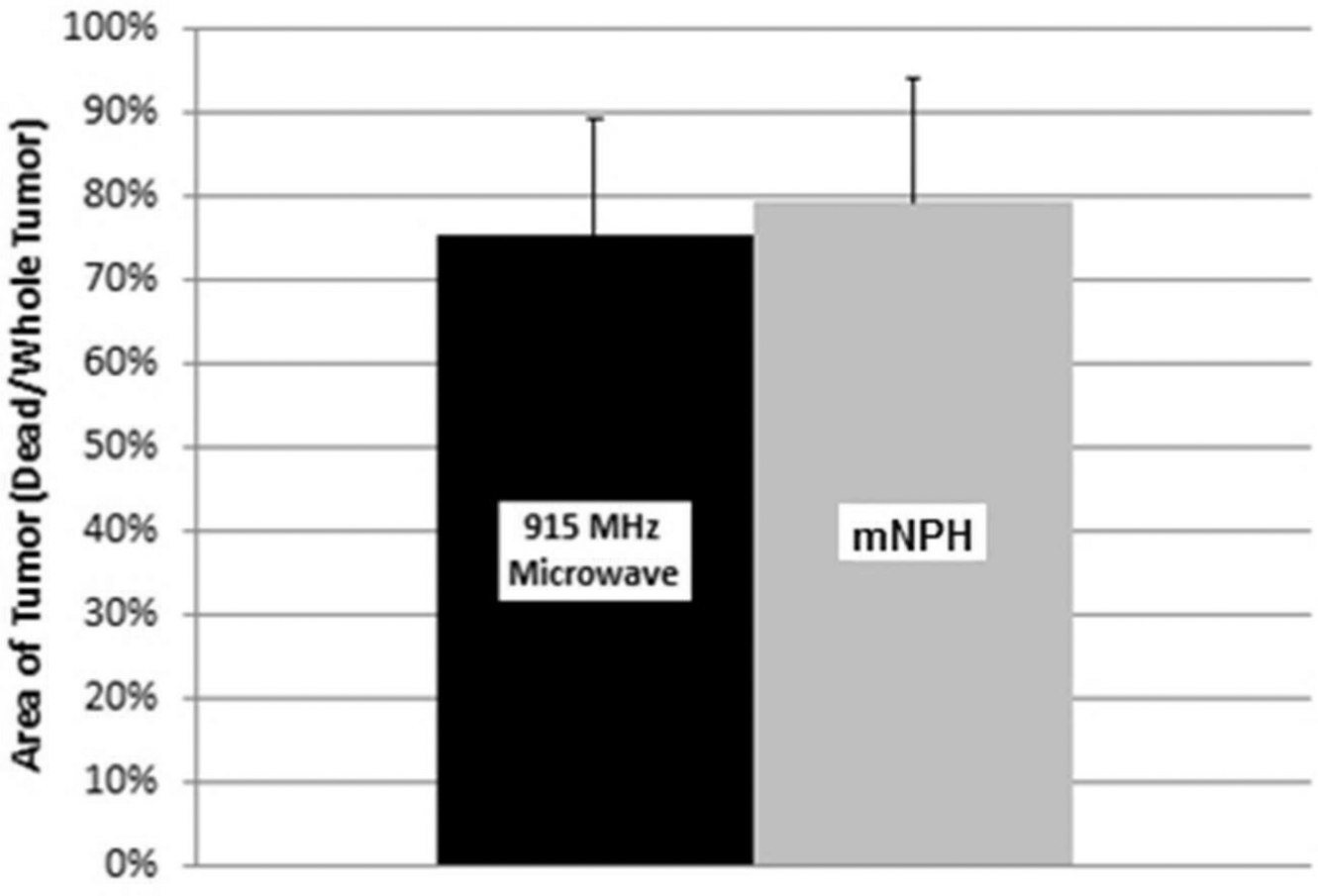

Figure 9.

This graph demonstrates a comparison of necrotic tumor area 24 hours following mNPH and microwave treatment (CEM 60). Histological evaluation of tumors treated with 915 MHz microwave hyperthermia show 75% of the tumor area is necrotic in comparison to mNPH (79% necrotic). Statistical significance between groups was not found (p=0.55). Error bars represent standard deviation. All tumors were evaluated 24 hours following treatment.

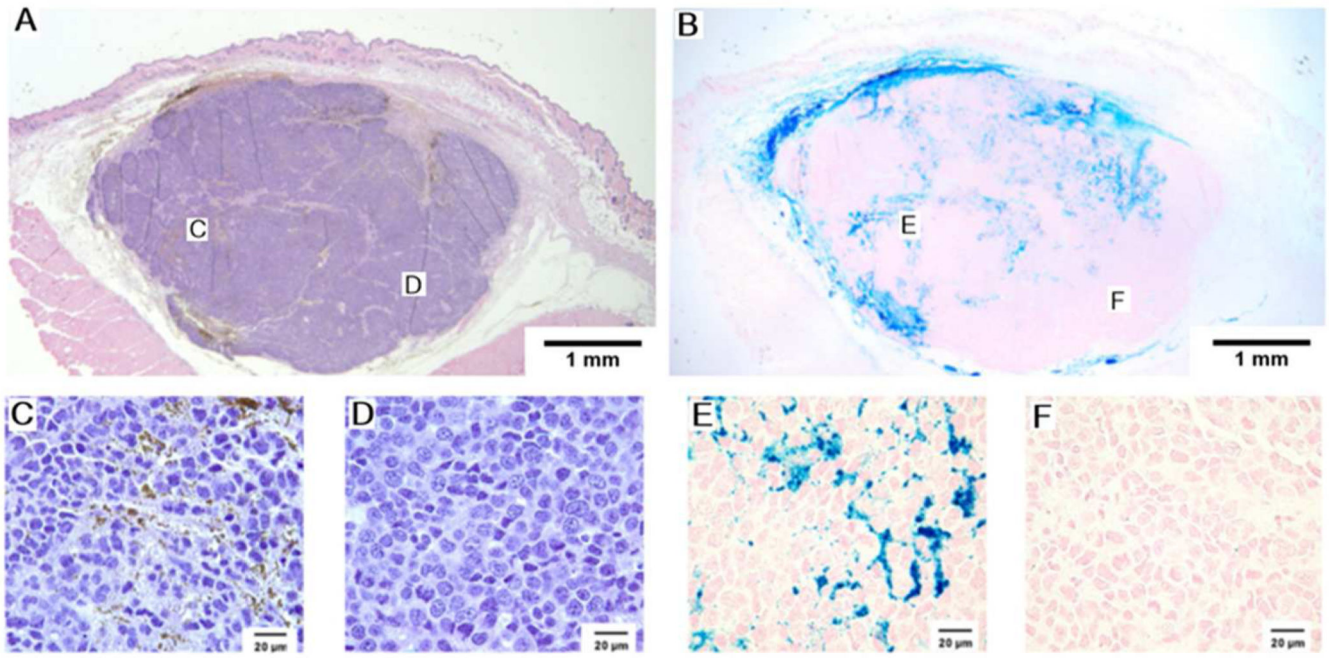

Figure 10.

A representative MTGB tumor with histologic sections taken five minutes after mNP injection. These H&E and Prussian blue photomicrographs demonstrate regional heterogeneity in mNP distribution. The 110 nm diameter mNP were injected in four tissue quadrants, with a total of 7.5 mg of Fe per cm^3 tumor, five minutes prior to tumor removal and processing. Regions indicated on the low magnification images are shown in the high magnification images. H&E and Prussian blue. A&B at 10× magnification, C,D,E, and F at 100× magnification.

Table 1

Summary of post-treatment tissue damage immediately beneath the tumor. Tissue was evaluated for the presence of edema, muscle necrosis and hemorrhage. Zones were 0.75 mm thick. Zone 1 began at the deep edge of the tumor. If no damage was observed, “normal tissue” was reported.

Mouse	Zone 1	Zone 2	Zone 3
MNPH 1	Edema	Edema	Normal Muscle
MNPH 2	Edema	Normal muscle	Normal Muscle
MNPH 3	Edema	Normal Muscle	Normal Muscle
MNPH 4	Edema	Normal Muscle	Normal Muscle
MNPH 5	Edema	Normal Muscle	Normal Muscle
MNPH 6	Normal Muscle	Normal Muscle	Normal Muscle
MNPH 7	Normal Muscle	Normal Muscle	Normal Muscle
MNPH 8	Edema	Edema	Normal Muscle
MNPH 9	Edema	Normal Muscle	Normal Muscle
915 MHz Microwave 1	Edema and hemorrhage	Edema and Necrotic Muscle	Necrotic Muscle
915 MHz Microwave 2	Edema	Normal Muscle	Normal Muscle
915 MHz Microwave 3	Hemorrhage	Necrotic Muscle and Edema	Normal Muscle
915 MHz Microwave 4	Edema and Necrotic Muscle	Normal Muscle	Normal Muscle
915 MHz Microwave 5	Necrotic Muscle	Necrotic Muscle	Normal Muscle
915 MHz Microwave 6	Edema and Necrotic Muscle	Edema and Necrotic Muscle	Normal Muscle
915 MHz Microwave 7	Necrotic Muscle	Necrotic Muscle	NA
915 MHz Microwave 8	Necrotic Muscle	Necrotic Muscle	NA
915 MHz Microwave 9	Necrotic Muscle	Necrotic Muscle	Necrotic Muscle